

Cell Reports, Volume 26

Supplemental Information

**A Late Phase of Long-Term Synaptic Depression
in Cerebellar Purkinje Cells
Requires Activation of MEF2**

Milena M. Andzelm, Devorah Vanness, Michael E. Greenberg, and David J. Linden

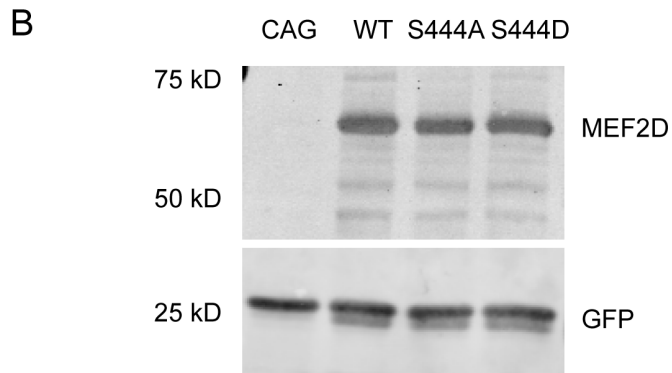
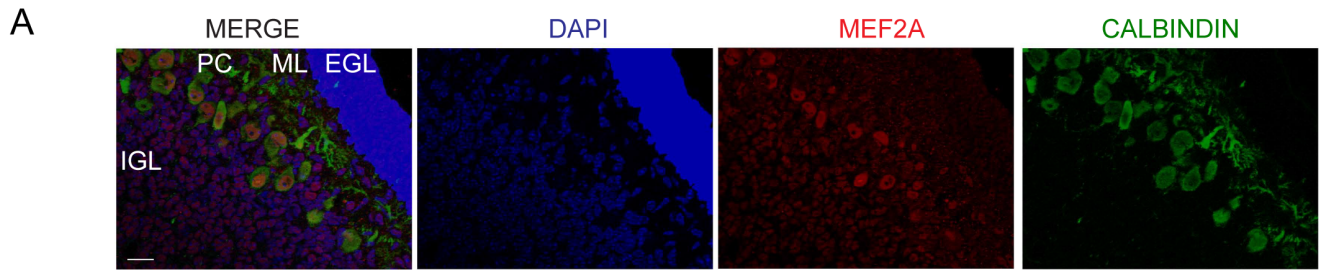


Figure S1. MEF2A expression in Purkinje cells and equal expression of MEF2D phosphomutant constructs (related to Figures 1 and 2). **A)** Immunofluorescence of MEF2A (red) and Calbindin (green) is shown in WT P11 mouse cerebellum. Shown is the internal granule cell layer (IGL), Purkinje cell layer (PC), molecular layer (ML) and external granule cell layer (EGL). **B)** Western blot of MEF2D and GFP in 293t cells transfected with equal amounts of the WT form of MEF2D, or phosphomutants S444A or S444D. Ratio of fluorescence intensity of MEF2D compared to GFP fluorescence was calculated, and then normalized to WT MEF2D/GFP ratio. Expression levels were not significantly different. Figure is representative of 3 independent experiments.

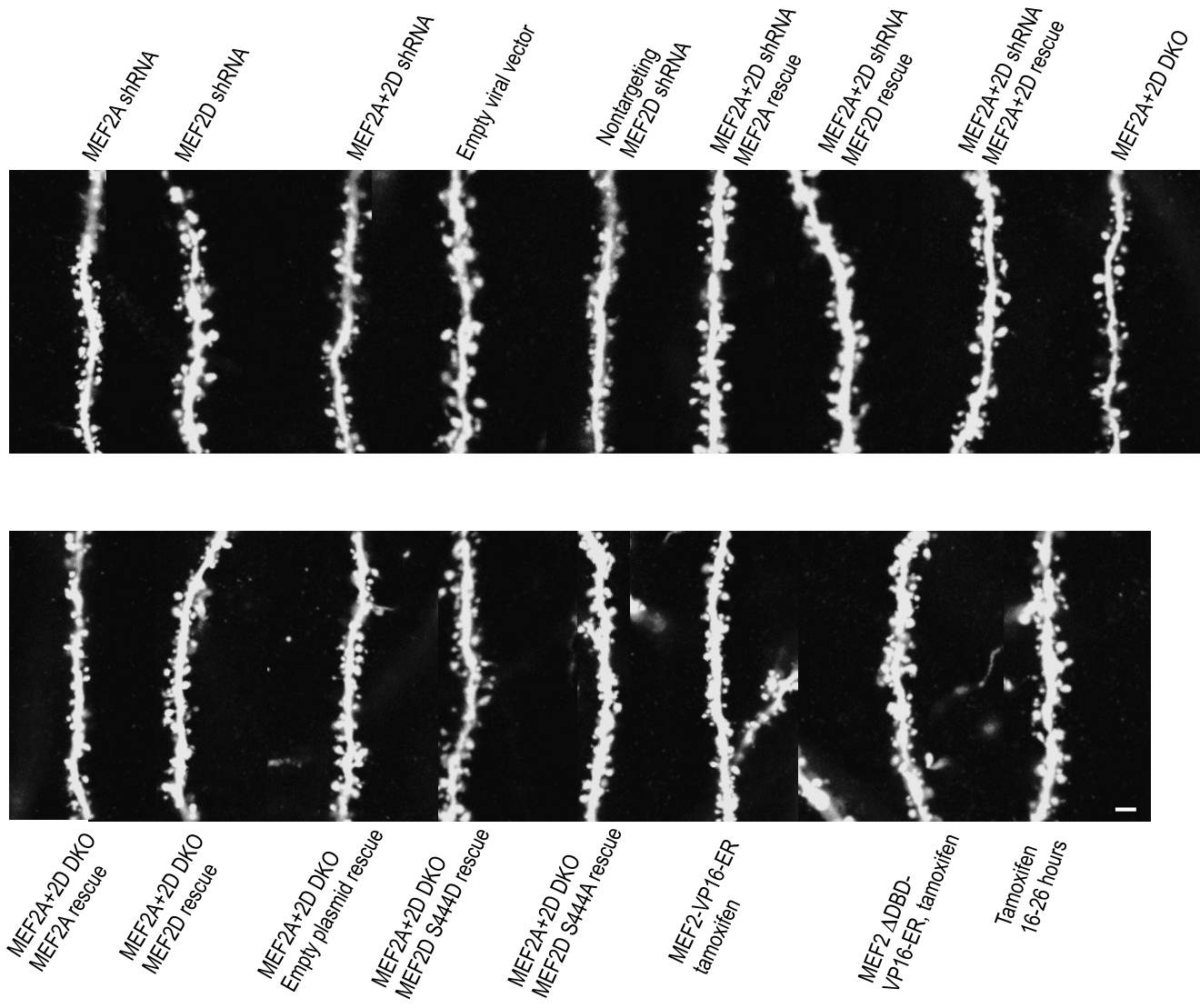


Figure S2. Dendritic fine structure is not altered by alterations of MEF2 used in this study (related to Figures 1, 2 and 3). This confocal image is a composite of exemplar mid-distal dendritic segments, each from a different cultured Purkinje cell on the day of recording. Fluorescence driven from a dsRedExpress marker plasmid is shown. Scale bar = 2 μ m. The population measures for spine density corresponding to these images may be found in Supplemental Table 1. Scale bar = 2 μ m.

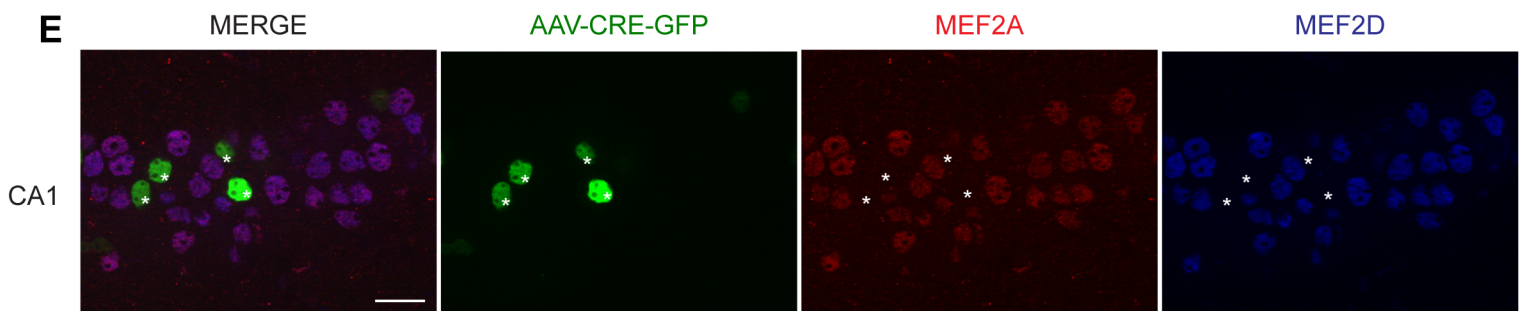
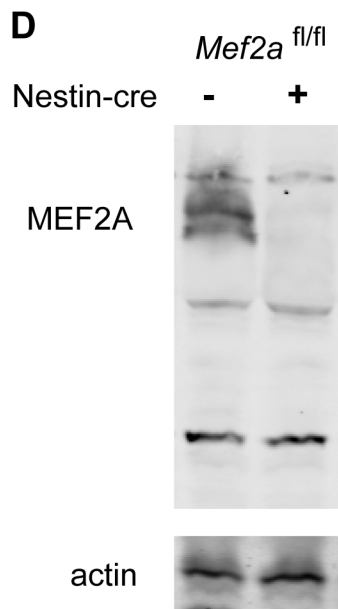
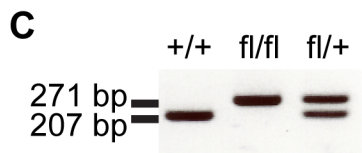
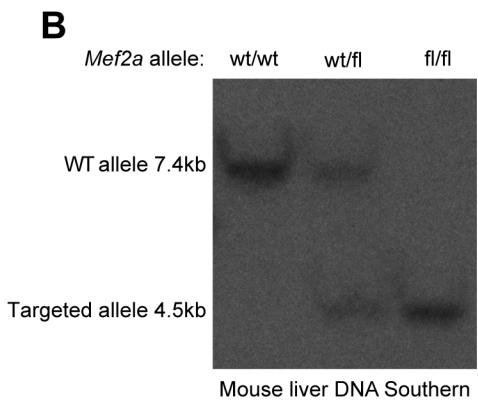
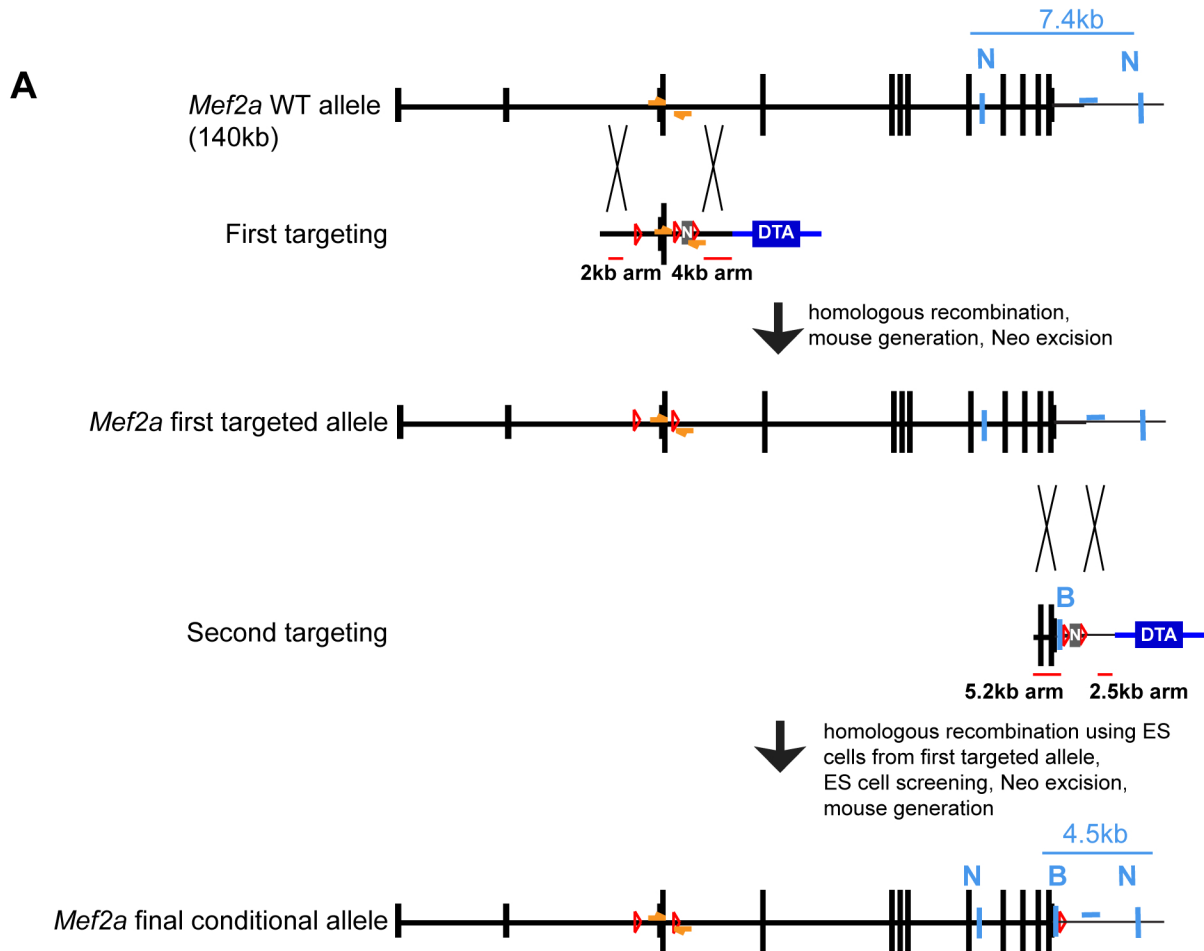


Figure S3. Generation and validation of a novel line of *Mef2a* conditional KO mice (related to Figure 2).

(A) Schematic of the *Mef2a* gene targeting strategy, not to scale. (Top) *Mef2a* WT allele aligned with the corresponding part of the first targeting construct. The first coding exon of the allele was flanked by loxP sequences (red triangles). A neomycin positive selection cassette (N) was inserted with a 3rd loxP site at the 3' end of the targeted region and Diphtheria toxin A (DTA) served as a negative selection marker. (Middle) Mice were generated from correctly targeted ES cells, Neomycin was excised and MEF2A deletion was assessed. Removal of the first coding exon was found to produce a large truncation product (data not shown). Therefore ES cells were generated from the targeted mice and a second targeting of the same allele was performed. In the second targeting a loxP site was inserted 3' to the final coding exon using the same positive and negative selection strategies as described above. (Bottom) ES cells were then assessed by long-range PCR for successful double targeting of the same allele (the presence of 3 loxP sites on the same allele, 2 at the 5' end and 1 on the 3' end of the coding region of the *Mef2a* allele) (data not shown). Successfully targeted ES cells were then injected into pseudopregnant females, and subsequent progeny were assessed for successful germline transmission of the targeted allele. Light blue boxes represent the relative position of the 3' southern blot probe, external to the targeted region, and southern blot enzyme digestion sites are denoted as N (NdeI) and B (BamHI). Distances between restriction sites for southern blot analysis are illustrated in light blue above the WT and targeted alleles. Orange arrows denote relative positions of PCR genotyping primers. (B) Southern blot analysis of NdeI and BamHI-digested genomic DNA from mouse liver DNA using a 3' probe (blue box in Figure S4A) indicates that mice carry the correctly targeted locus. Expected genomic DNA fragment lengths are illustrated in Figure S1A above. (C) Polymerase chain reaction (PCR) results for routine genotyping of *Mef2a^{fl/fl}* mice. Genotyping for the conditional *Mef2a* allele was performed by PCR using primer pairs F (5'-gctttaactgatatcttttaggacca-3') and R (5'-caccaaagattatgcccact-3') which span the 3' loxP site introduced in the first targeting (schematized in Figure S1A, orange arrows). (D,E) Effective removal of MEF2A using Cre recombinase. (D) Western blot of MEF2A in whole brain lysates of a *Mef2a^{fl/fl}* mouse expressing Nestin-cre and a littermate *Mef2a^{fl/fl}* mouse with no Cre. Actin was used as a loading control. (E) Immunofluorescence of MEF2D (blue) and MEF2A (red) in CA1 hippocampal neurons of *Mef2a^{fl/fl}* *Mef2a^{fl/fl}* mice injected with an AAV expressing CRE-GFP at P20 and harvested at P26 (white asterisks designate examples of cells expressing CRE-GFP). Scale bar = 20µm.

Manipulation	basal Ca, nM	depol-evoked Ca	DHPG-evoked Ca	spine density, / μm	soma area, μm^2
MEF2A shRNA	130 \pm 24	557 \pm 54	270 \pm 37	1.4 \pm 0.3	113 \pm 20
MEF2D shRNA	110 \pm 30	509 \pm 45	256 \pm 38	1.1 \pm 0.3	127 \pm 21
MEF2A+2D shRNA	118 \pm 23	532 \pm 60	221 \pm 28	1.2 \pm 0.3	119 \pm 16
Empty viral vector	129 \pm 28	600 \pm 67	270 \pm 36	1.2 \pm 0.3	114 \pm 25
Nontargeting MEF2D shRNA	105 \pm 22	551 \pm 50	219 \pm 33	1.5 \pm 0.4	122 \pm 20
MEF2A+2D shRNA, MEF2A rescue	126 \pm 22	553 \pm 60	206 \pm 32	1.3 \pm 0.3	110 \pm 24
MEF2A+2D shRNA, MEF2D rescue	110 \pm 27	538 \pm 58	237 \pm 36	1.3 \pm 0.2	131 \pm 28
MEF2A+2D shRNA, MEF2A+2D rescue	129 \pm 26	572 \pm 56	245 \pm 29	1.5 \pm 0.3	115 \pm 19
MEF2A+2D DKO	104 \pm 20	517 \pm 66	230 \pm 35	1.3 \pm 0.4	127 \pm 26
MEF2A+2D DKO, MEF2A rescue	118 \pm 30	613 \pm 76	247 \pm 38	1.2 \pm 0.4	120 \pm 24
MEF2A+2D DKO, MEF2D rescue	123 \pm 26	554 \pm 54	228 \pm 31	1.3 \pm 0.3	113 \pm 27
MEF2A+2D DKO, empty plasmid rescue	114 \pm 26	537 \pm 67	218 \pm 35	1.4 \pm 0.3	126 \pm 22
MEF2A+2D DKO, MEF2D S444D rescue	120 \pm 27	568 \pm 63	263 \pm 31	1.6 \pm 0.4	119 \pm 24
MEF2A+2D DKO, MEF2D S444A rescue	117 \pm 30	604 \pm 54	254 \pm 24	1.4 \pm 0.3	113 \pm 23
MEF2-VP16-ER, tamoxifen	119 \pm 25	499 \pm 45	227 \pm 28	1.3 \pm 0.3	129 \pm 25
MEF2 Δ DBD-VP16-ER, tamoxifen	114 \pm 22	532 \pm 51	235 \pm 23	1.2 \pm 0.3	110 \pm 18
Tamoxifen, 16-26 hours	124 \pm 19	490 \pm 61	245 \pm 26	1.5 \pm 0.4	119 \pm 27

Table S1. The MEF2 shRNAs, expression constructs and mutant mice used in this study do not have unintended side-effects on basal Ca concentration, depolarization-evoked or mGlu1 agonist-evoked dendritic Ca transients, dendritic spine density or somatic area in cultured Purkinje cells (related to Figures 1, 2 and 3).

Purkinje cells were pipette-loaded with a Cs-based internal saline supplemented with bis-fura-2 (100 μM) to allow for dendritic Ca imaging after 25 min of equilibration in whole cell mode. Voltage-clamped Purkinje cells were challenged with step depolarization to 0 mV (1 s duration), or a micropressure pulse of the mGluR1/5 agonist DHPG (10 psi, 2 s) as an index of voltage-sensitive Ca channel function and mGluR1 function, respectively. $n = 10$ cells/group. Spine density and soma area were measured from 20 Purkinje cells in each group using confocal imaging of fluorescence derived from a dsRed2 marker plasmid (see Figure S3 for exemplar images).